

# Reverse Monte Carlo neutron scattering study of the “ordered-ice” oxide pyrochlore $\text{Pb}_2\text{Ru}_2\text{O}_{6.5}$

**Daniel P. Shoemaker**

Materials Science Division, Argonne National Laboratory  
Argonne, IL, 60439, USA

E-mail: [dshoemaker@anl.gov](mailto:dshoemaker@anl.gov)

**Anna Llobet**

Lujan Neutron Scattering Center, Los Alamos National Laboratory  
MS H805, Los Alamos, NM 87545, USA

E-mail: [allobet@lanl.gov](mailto:allobet@lanl.gov)

**Makoto Tachibana**

National Institute for Materials Science  
Namiki 1-1, Tsukuba, Ibaraki 305-0044, Japan

E-mail: [TACHIBANA.Makoto@nims.go.jp](mailto:TACHIBANA.Makoto@nims.go.jp)

**Ram Seshadri**

Materials Department and Materials Research Laboratory  
University of California, Santa Barbara, CA, 93106, USA

E-mail: [seshadri@mrl.ucsb.edu](mailto:seshadri@mrl.ucsb.edu)

**Abstract.** We employ high-resolution total neutron scattering in conjunction with reverse Monte Carlo simulations to examine, in a detailed and unbiased manner, the crystal structure of the vacancy-ordered oxide pyrochlore  $Pb_2Ru_2O_6O'_{0.5}$  in light of its structural analogy with proton-ordering in the structures of ice. We find that the vacancy and the  $O'$  ion are completely ordered, and that the average structure in the  $F\bar{4}3m$  space group describes the vacancy ordering precisely. We complement these results with an examination of the  $Pb^{2+}$  lone pair network using density functional electronic structure calculations, and a comparison of the low-temperature lattice-only heat capacity of  $Pb_2Ru_2O_6O'_{0.5}$  with that of other related pyrochlores.

PACS numbers: 61.05.fm, 61.43.Bn,

## 1. Introduction

In recent years, pyrochlore[1]  $A_2B_2O_6O'$  compounds (also described compactly as  $A_2B_2O_7$ ) have been explored – in cases where A is a rare-earth ion and B is a transition element – for a number of reasons ranging from their unusual magnetic “spin-ice” ground states[2] and their anomalous Hall effect behavior[3] to possible realization of magnetic monopoles,[4] and because certain pyrochlore compositions, notably  $Y_2Ir_2O_7$ , can display electron correlation in the presence of spin-orbit coupling.[5]

When pyrochlores are prepared with lone-pair active ions such as  $Pb^{2+}$  or  $Bi^{3+}$  on their A sites, rather than rare-earth or alkaline earth ions, one can expect interesting structural effects. An example of this is the grotesquely complicated low-temperature structure of  $Bi_2Sn_2O_7$  and its numerous polymorphs that form upon heating.[6, 7] Hector and Wiggin[8] reported a low-temperature preparation of  $Bi_2Ti_2O_6O'$  in 2004; a compound which prefers to disorder extensively and locally, and remains cubic down to a temperature of 2 K rather than undergo a phase transition to a coherently disordered ground state. This observation led to the suggestion that just as the pyrochlore lattice hinders coherent magnetic ordering[9] so too possibly are coherent lone-pair induced displacements hindered in compounds such as  $Bi_2Ti_2O_6O'$  and related pyrochlores[10, 11, 12] a phenomenon dubbed “charge-ice”[13] in analogy with problems of proton ordering in the structure of ice- $I_c$  and ice- $I_h$ . [14, 15] The low-temperature thermal properties[16] and detailed scattering studies [17] have supported the validity of this suggestion.

In contrast to  $A_2B_2O_6O'$  pyrochlores, which crystallize in the  $Fd\bar{3}m$  space group and whose  $O'$  sites describe a diamond lattice, in  $Pb_2Ru_2O_6O'_{0.5}$  (average structure reported from Rietveld refinements of neutron[18] and synchrotron X-ray diffraction[19]) there is ordering of  $O'$  and a vacancy (depicted by  $\square$ ) so that the compound crystallizes in the  $F\bar{4}3m$  subgroup of  $Fd\bar{3}m$ , with  $O'$  and  $\square$  forming a zinc blende lattice. The complete ordered structure in space group  $F\bar{4}3m$  can be written  $A_2B_2O_{12}O'\square$ . In contrast to  $A_2B_2O_6O'$  where the diamond  $O'$  lattice has an A ion between every two  $O'$ , in  $A_2B_2O_{12}O'\square$ , each A ion has an  $O'$  and a  $\square$  as neighbors, at least in the perfectly ordered structure (slightly further are six O neighbors in the  $B_2O_6$  sublattice).

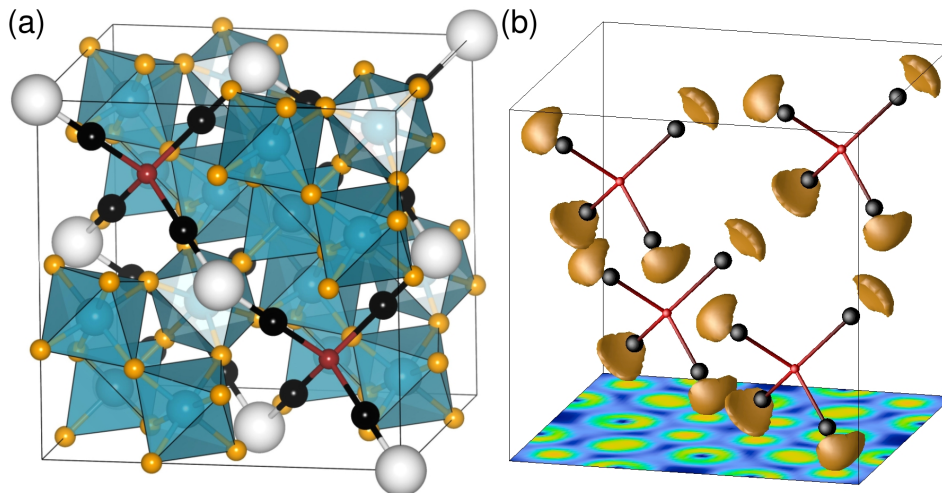


**Figure 1.** (Color online) (a) The unit cell of  $Pb_2Ru_2O_6O'_{0.5}$  consisting of corner-sharing networks of  $RuO_6$  octahedra and isolated  $O'Pb$  tetrahedra. The ordered vacancies ( $\square$ ) are in the  $4a(0,0,0)$  positions and are indicated using large white spheres. (b) The lone-pairs on the  $Pb^{2+}$  visualized using electron localization function at an isosurface of 0.80. For clarity, Ru and O are not displayed in (b).

The analogy with ice arises in the following manner: the topology of  $A_2O'$  in the pyrochlore structure is analogous to the topology of  $H_2O$  in ice  $I_c$ , with the protons in the latter obeying the “2-in, 2-out” Bernal-Fowler rules[14] in a completely random way that results in residual entropy.[15, 20] If the title compound were fully ordered, the  $A_2(O'\square)_{0.5}$  network would also be completely ordered with the A ions ( $Pb^{2+}$ ) choosing to all bond to  $O'$  or to  $\square$  in a “4-in 0-out” fashion. Hence our use of the term “ordered-ice”. Figure 1(a) displays the crystal structure of completely vacancy-ordered  $Pb_2Ru_2O_6O'_{0.5}$ . The vacancy sites are displayed as large white spheres in order to emphasize the  $Pb^{2+}(O'\square)_{0.5}$  network in the structure.

In this contribution, we employ high-resolution neutron scattering tools based on analysis using the reverse Monte Carlo method[21, 22] and least-squares refinements to establish, in a structurally unbiased manner, the extent of ordering between  $O'$  and  $\square$ . We find that the average structural description in the  $F43m$  space group of completely ordered vacancies is consistent with the results of the reverse Monte Carlo simulation of total scattering. An interesting consequence of the ordered vacancies is that the stereochemically active lone pairs on the  $Pb^{2+}$  ions have a location to position themselves in a completely coherent fashion as we shall show. We use this study to emphasize the importance of employing *both* the Bragg scattering intensity as well as the pair distribution function,  $G(r)$  in the reverse Monte Carlo analysis. Finally, we examine the lattice part of the low temperature heat capacity for local Einstein modes that have been observed in other pyrochlore compounds with incoherent lone pairs.[11, 23]

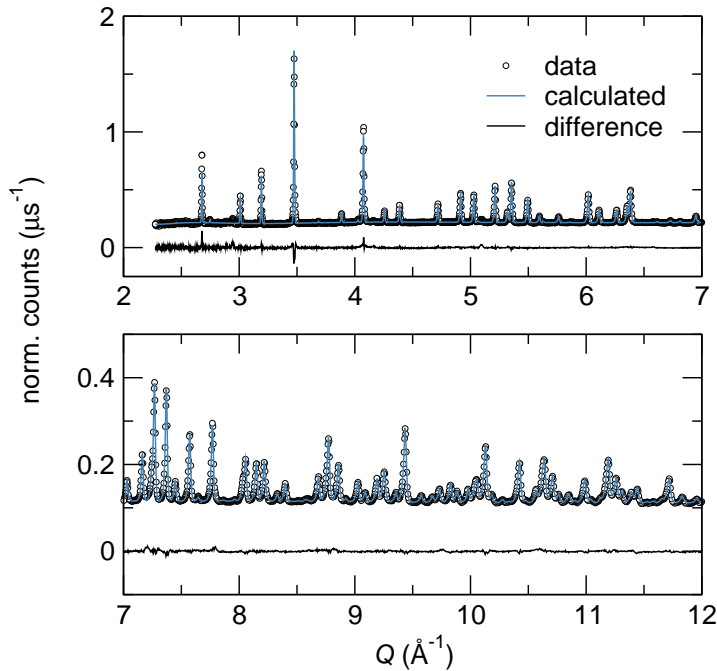


**Figure 2.** (Color online) The neutron TOF Rietveld refinement for  $\text{Pb}_2\text{Ru}_2\text{O}_{6.5}$  at  $T = 15\text{ K}$  confirms the  $F\bar{4}3m$  space group. The data is presented in two panels to emphasize the  $Q$ -range and the quality of the fit.

## 2. Experimental and computational Methods

The sample for neutron scattering was obtained by careful crushing and grinding of  $\text{Pb}_2\text{Ru}_2\text{O}_6\text{O}'_{0.5}$  single crystals, whose average structure by synchrotron X-ray Rietveld refinement, and whose electrical transport properties have been previously reported.[19] Time-of-flight (TOF) total neutron scattering was carried out at the NPDF instrument at Los Alamos National Laboratory at 300 K and 15 K. Rietveld refinement was performed with the EXPGUI frontend for GSAS.[24]. Extraction of the PDF  $G(r)$  with PDFGETN[25] used  $Q_{max} = 35 \text{ \AA}^{-1}$ . Reverse Monte Carlo simulations were run using RMCPROFILE version 6 [22] and a  $6 \times 6 \times 6$  unit cell with 18144 atoms. These simulations were simultaneously constrained by the Bragg profile and the  $G(r)$ . Multiple runs were performed and averaged when necessary to obtain the most accurate representation of the fit to data. First principles electronic structure visualization made use of the linear muffin-tin orbital method within the atomic sphere approximation using version 47C of the Stuttgart TB-LMTO-ASA program.[26] More details of such calculations in Pb and Bi-based pyrochlore oxides can be found in reference [13].

## 3. Results and discussion

The result of Rietveld refinement using neutron TOF scattering is shown in Fig. 2. No impurities are present, and the  $F\bar{4}3m$  unit cell provides an excellent fit, with details into the high- $Q$  range reproduced past  $Q = 12 \text{ \AA}^{-1}$ . This model contains Pb atoms that

**Table 1.** Average structural parameters for  $Pb_2Ru_2O_6O'_{0.5}$  obtained from Rietveld refinement of TOF neutron diffraction data in the space group  $F\bar{4}3m$  (No. 216).  $a = 10.25017(2)$  Å/ at 300 K and  $a = 10.22775(2)$  Å at 15 K. All sites refine to full occupancy.

$T = 300$ K					
atom	site	$x$	$y$	$z$	$U_{iso}$ (Å <sup>2</sup> )
Pb	16e	0.8766(1)	$x$	$x$	0.0117(1)
Ru	16e	0.3748(1)	$x$	$x$	0.0057(1)
O1	24f	0.3053(2)	0	0	0.0105(4)
O2	24g	0.4502(2)	$\frac{1}{4}$	$\frac{1}{4}$	0.0082(3)
O'	4d	$\frac{3}{4}$	$\frac{3}{4}$	$\frac{3}{4}$	0.0089(3)
□	4a	0	0	0	–
$T = 15$ K					
atom	site	$x$	$y$	$z$	$U_{iso}$ (Å <sup>2</sup> )
Pb	16e	0.87725(8)	$x$	$x$	0.00377(8)
Ru	16e	0.3747(1)	$x$	$x$	0.00299(8)
O1	24f	0.3039(1)	0	0	0.0063(2)
O2	24g	0.4504(1)	$\frac{1}{4}$	$\frac{1}{4}$	0.0042(3)
O'	4d	$\frac{3}{4}$	$\frac{3}{4}$	$\frac{3}{4}$	0.0051(2)
□	4a	0	0	0	–

are shifted off the ideal pyrochlore  $A$  site into a 16e position at  $(x, x, x)$ . The  $O'$  anions occupy 4d sites. Details of the structure obtained from Rietveld refinement of the 300 K and 15 K data are displayed in Table 1. All atoms refine to their full occupancy and all the isotropic thermal parameters from the refinement refine to acceptable values.

With the ideal, average structure, density functional calculations can be performed, and used to locate the lone pairs on  $Pb^{2+}$  [27] using the electron localization function (ELF). [28, 29] Figure 1(b) displays the lone pair network, visualized for an isosurface value of  $ELF = 0.80$ . The lone pairs on  $Pb^{2+}$  are seen to coherently dispose themselves in the direction of the □. It is interesting to note that while lone pairs are known to possess a volume that is comparable to that of oxide anion, the lone pair to nucleus (of  $Pb^{2+}$ ) distance is significantly smaller than the distance from  $Pb^{2+}$  to  $O'$ . Hence, the lone pairs are not actually located in the vacant □ site at  $4a(0, 0, 0)$ . This is in keeping with the empirical findings of Galy, Andersson and others. [30] It is instructive to compare this ordered lone pair arrangement with what is seen in “charge-ice”  $Bi_2Ti_2O_6O'$ . In  $Bi_2Ti_2O_6O'$ , which has no vacant site, the lone pairs are obliged to displace perpendicular to the  $O'-A-O'$  axis, and they do so incoherently, with profound structural and thermodynamic consequences. [13, 16, 17]

Manually altering the Pb positions or  $O'$  ordering in the model reveals that both of these values are strongly constrained by the data. In Fig. 3 the effect on the goodness-of-fit  $\chi^2$  is plotted as a function of Pb displacement. For an ideal pyrochlore cell, the

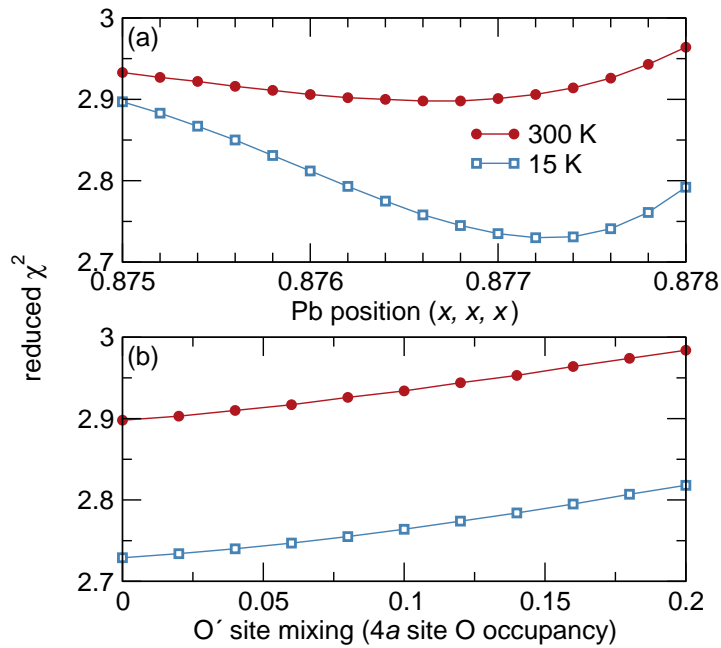


**Figure 3.** (Color online) In (a), moving Pb off of its refined position at  $x = 0.8766$  results in a poorer fit, seen from the poorer fit (larger  $\chi^2$ ) for data acquired at 15 K and 300 K. In (b), O' occupancy perfectly ordered (left) and increased to simulate disorder spilling onto the vacant sites. Again, even small amounts of disordered O' give a poorer Rietveld refinement.

Pb would lie at the left-most end of the plot with  $x = \frac{7}{8} = 0.875$ . Refinements at  $T = 15$  K and 300 K both suggest Pb positions near 0.877, which are about 0.04 and 0.03 Å displaced, respectively, off their ideal sites and away from the nearby O'.

Moving fractional O' occupancy onto the 4a vacant  $\square$  site in our model is equivalent to introducing site disorder, where having full occupancy on both sites would mimic the O' sublattice of the full pyrochlore structure. The effect of increasing O' occupancy on the  $\square$  site (with corresponding decrease at the O' 4d position) is seen in Fig. 3(b). Again, any occupancy on 4a results in an increased  $\chi^2$ , implying that Bragg scattering supports O' being fully ordered, even at 300 K. This strong proclivity to order the O' and, in turn, the Pb displacements, is seen in related solid solutions  $Pb_{2-x}Ln_xRu_2O_{7-y}$  ( $Ln = Nd, Gd$ ) which can tolerate only a small amount ( $x < 0.2$ ) of A-site substitution before the disorder drives formation of a separate  $Fd\bar{3}m$  phase. [31]

The quality of the fit to the Rietveld-refined structure and the stabilities of the Pb position and O' ordering provide evidence that  $Pb_2Ru_2O_6O'_{0.5}$  appears structurally to be consistent with the unit cell, unlike the full-O' pyrochlores such as  $Bi_2Ti_2O_6O'$  where the difficulty in accommodating the lone pairs results in incoherent structural disorder and off-centering. In  $Bi_2Ti_2O_6O'$ , local structure analysis reveals details of the short-range structure that are difficult to determine from average structure probes that rely on Bragg scattering alone. In a system such as  $Pb_2Ru_2O_6O'_{0.5}$  where structural frustration should be removed by O' ordering, it is of interest to ask whether the local structure

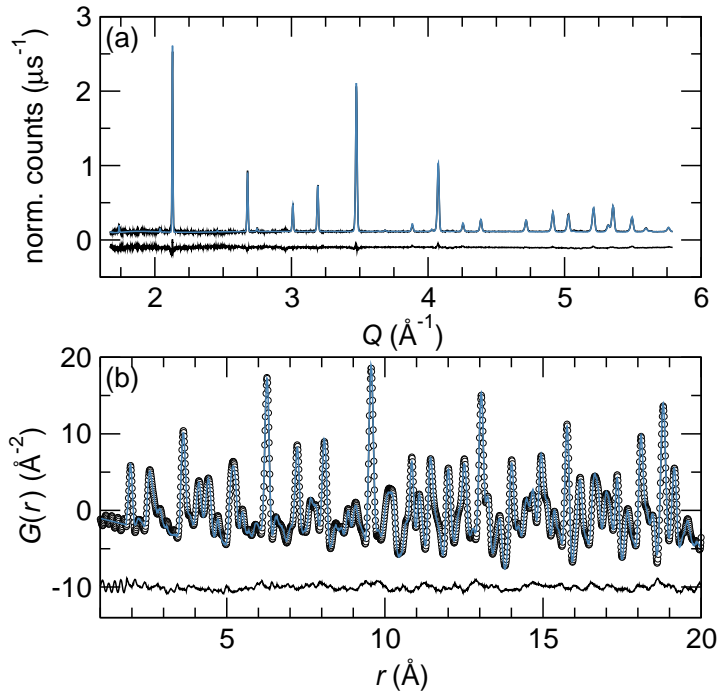


**Figure 4.** (Color online) Reverse Monte Carlo (RMC) fits to the Bragg profile (a) and  $G(r)$  (b) obtained from neutron total scattering at 15 K. Pair correlations are extracted from these RMC supercells.

exhibits any hallmarks of a disordering that is not seen in the Bragg scattering/Rietveld analysis.

Reverse Monte Carlo fits to the neutron TOF total scattering are shown in Fig. 4. The Bragg profile retains the long-range periodicity and average atomic displacement parameters of the structure, while the  $G(r)$  constrains pairwise distances and reproduces the local structure. By simultaneously fitting both datasets, we are left with a large supercell that provides a snapshot of the material. Structural details of this model can be analyzed statistically to determine the precise local tendencies supported by the experimental data.

The partial pair distribution functions in Fig. 5(a) display the Pb–O' distances in the unit cell  $n_{Pb-O'}(r)$  and the distances of Pb to the vacant site  $n_{Pb-\square}(r)$ . The shift versus  $r$  shows that Pb–O' distances are longer, so Pb nuclei have displaced off their ideal site toward the vacant  $\square$  position.

Partial pair distribution functions can also reveal ordering on the O' sublattice when vacancy “atoms” with zero scattering cross-section are placed on the vacant O' positions. The vacancies are freely allowed to swap with O' during the RMC simulation. For a simultaneous fit to Bragg peaks and the  $G(r)$ , ordering is retained: the  $r = 4.45$  Å nearest-neighbor distance between occupied and vacant O' sites has no intensity for the  $n_{O'-O'}(r)$  distribution in Fig. 5(b), indicating that no two O' atoms share neighboring sites. However, if the RMC simulation is performed as a fit to the  $G(r)$  only (and the Bragg profile is ignored) then the O' ordering begins to melt and O' can be found on the

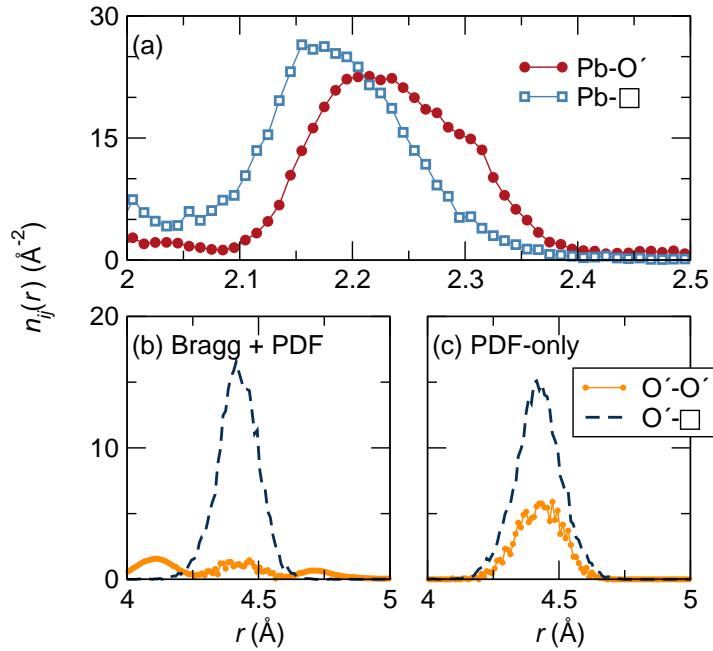


**Figure 5.** (Color online) In (a), pair correlations from the RMC supercell show the Pb–O’ and Pb–vacancy distances. The peaks are offset, indicating a shift of Pb toward O’. In (b), O’–O’ and O’–vacancy pair correlations show that O’ are ordered when RMC simulations are constrained by the  $G(r)$  and Bragg profile. A fit unconstrained by Bragg scattering (c) becomes partially disordered on the O’–vacancy sublattice—the  $G(r)$  is insufficient to reproduce the ordered distribution via RMC.

vacancy sites, as seen in Fig 5(c). Both models are, at some level, “correct” because they reproduce the respective experimental data. However, the data guiding the  $G(r)$ -only fit is incomplete. The O’ ordering prescribed by the Bragg pattern and verified in Fig. 3(b) is unambiguous, so the fully ordered case is confirmed. Because RMC is a stochastic technique, it reveals that the  $G(r)$  alone does not contain sufficiently robust information about the O’ occupancy to prevent O’ from spilling onto disordered sites. Only when the additional Bragg constraint is applied is the fully ordered model reproduced from the data.

Finally, it is of interest to see whether the ordered arrangement of  $Pb^{2+}$  ions and their associated lone pairs result in distinctly different low-temperature heat capacity behavior in  $Pb_2Ru_2O_6O'_{0.5}$  when compared to a compound with disordered lone pairs such as  $Bi_2Ti_2O_6O'$ . We display such a comparison in Fig. 6. The scheme used to display the scaled heat capacity,  $C_p/T^3$  vs.  $T$  allows local Einstein-like modes to be distinguished,[33] and the temperature of the peak(s) can be read off as energies of the Einstein mode. Liu and Löhneysen[34] have suggested a general scaling law wherein the lower the temperature at which  $C_p/T^3$  displays a maximum, the larger the peak height as well. They have made such correlations for a number of amorphous and crystalline systems and  $Bi_2Ti_2O_6O'$  (with its highly disordered  $Bi_2O'$  network[17]) displays, of all studied crystalline systems, one of the lowest peak temperatures and largest peak



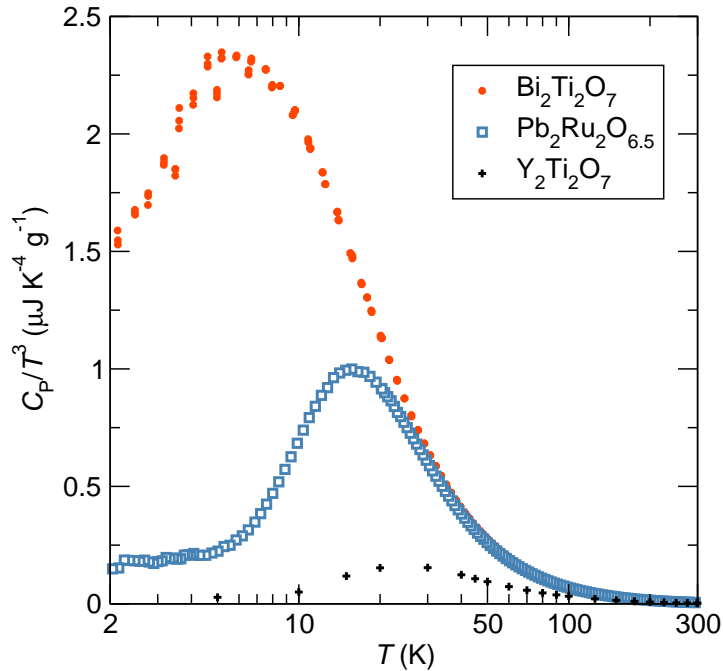


**Figure 6.** (Color online) Lattice-only heat capacity, with the electronic contribution subtracted, of  $Pb_2Ru_2O_{6.5}$ , displayed in a manner that emphasizes Einstein-like features at low temperatures. For comparison, the similarly scaled heat capacity of “charge-cc”  $Bi_2Ti_2O_6O'$  (from reference [16]) and of pyrochlore  $Y_2Ti_2O_7$  (taken from reference [32]) which does not have lone pairs, is also displayed.

amplitudes. In contrast, we see from Fig. 6 that in  $Pb_2Ru_2O_{6.5}$ , (using published data from reference [19] after subtracting the electronic  $\gamma T$  contribution) the peak occurs at significantly higher temperatures and is significantly smaller in amplitude. It is nonetheless larger than what is seen for  $Y_2Ti_2O_7$ [32] which has no lone pairs. The question is why, in a completely ordered structure, is there an Einstein-like mode at all? The suggestion made recently by Safarik *et al.*[35] is that Einstein-like modes appear even in crystalline materials when van Hove peaks in the phonon densities of state cross the chemical potential. In any event, the trend seen in Fig. 6 is consistent with the finding that  $Pb_2Ru_2O_{6.5}$  has a well-ordered network of A-site atoms unlike  $Bi_2Ti_2O_6O'$ .

#### 4. Conclusions

Our study of the ordered-ice pyrochlore  $Pb_2Ru_2O_{6.5}$  has found that Rietveld refinements dictate  $O'-\square$  occupancy to be fully ordered, and  $Pb^{2+}$  is displaced toward  $O'$  (0.04 Å at  $T = 15$  K). This ordering implies that  $Pb_2Ru_2O_{6.5}$  does not possess the same geometric frustration seen in fully-occupied  $A_2B_2O_7$  pyrochlores with lone-pair active cations on the A sites. To compare  $Pb_2Ru_2O_{6.5}$  to those systems, where local structure analysis provide a view of incoherent distortions, we performed RMC simulations which revealed the presence of *coherent*  $Pb^{2+}$  off-centering only.

Simultaneous fits to the Bragg intensity and  $G(r)$  are required to reproduce the vacancy ordering, which is not strongly constrained by the  $G(r)$  alone. First-principles calculations and heat capacity measurements corroborate to show that the O'-□ ordering provides an outlet for (and perhaps is constrained by) the pointing of lone pairs into vacant  $4a$  positions.

## 5. Acknowledgments

We thank Joan Siewenie for assistance with data collection at NPDF. DPS and RS gratefully acknowledge support from the UCSB-LANL Institute for Multiscale Materials Studies, and from the National Science Foundation (DMR 0449354). DPS additionally acknowledges work at Argonne National Laboratory supported by the U.S. DOE, Office of Science, under Contract DE-AC02-06CH11357. This work made use of MRL Central Facilities, supported by the MRSEC Program of the NSF (DMR05-20415), a member of the NSF-funded Materials Research Facilities Network ([www.mrfn.org](http://www.mrfn.org)). NPDF at the Lujan Center at Los Alamos Neutron Science Center is funded by the DOE Office of Basic Energy Sciences and operated by Los Alamos National Security LLC under DOE Contract DE-AC52-06NA25396. RMC simulations were performed on the Hewlett Packard QSR cluster at the CNSI-MRL High Performance Computing Facility.

- [1] Subramanian M A, Aravamudan G and Rao G V S 1983 *Prog. Solid State Chem.* **15** 55–143
- [2] Ramirez A P, Hayashi A, Cava R J, Siddharthan R and Shastry B S 1999 *Nature* **399** 333–335
- [3] Taguchi Y, Oohara Y, Yoshizawa H, Nagaosa N and Tokura Y 2001 *Science* **291** 2573–2576
- [4] Morris D J P, Tennant D A, Grigera S A, Klemke B, Castelnovo C, Moessner R, Czternasty C, Meissner M, Rule K C, Hoffmann J, Kiefer K, Gerischer S, Slobinsky D and Perry R S 2009 *Science* **326** 411–414
- [5] Singh R S, Medicherla V R R, Maiti K and Sampathkumaran E V 2008 *Phys. Rev. B* **77** 201102
- [6] Evans I R, Howard J A K and Evans J S O 2003 *J. Mater. Chem.* **13**(9) 2098–2103
- [7] Shannon R D, Bierlein J D, Gillson J L, Jones G A and Sleight A W 1980 *J. Phys. Chem. Solids* **41** 117–122
- [8] Hector A L and Wiggin S B 2004 *J. Solid State Chem.* **177** 139–145
- [9] Ramirez A P 1994 *Ann. Rev. Mater. Sci.* **24** 453–80
- [10] Avdeev M, Haas M K, Jorgensen J D and Cava R J 2002 *J. Solid State Chem.* **169** 24–34
- [11] Melot B, Rodriguez E, Proffen T, Hayward M and Seshadri R 2006 *Mater. Res. Bull.* **41** 961–966
- [12] Henderson S J, Shebanova O, Hector A L, McMillan P F and Weller M T 2007 *Chem. Mater.* **19** 1712–1722
- [13] Seshadri R 2006 *Solid State Sci.* **8** 259–266
- [14] Bernal J D and Fowler R H 1933 *J. Chem. Phys.* **1** 514–548
- [15] Pauling L 1935 *J. Am. Chem. Soc.* **57** 2680
- [16] Melot B C, Tackett R, O'Brien J, Hector A L, Lawes G, Seshadri R and Ramirez A P 2009 *Phys. Rev. B* **79** 224111(1–5)
- [17] Shoemaker D P, Seshadri R, Hector A L, Llobet A, Proffen T and Fennie C J 2010 *Phys. Rev. B* **81** 144113
- [18] Beyerlein R, Horowitz H, Longo J, Leonowicz M, Jorgensen J and Rotella F 1984 *J. Solid State Chem.* **51** 253–265

- [19] Tachibana M, Kohama Y, Shimoyama T, Harada A, Taniyama T, Itoh M, Kawaji H and Atake T 2006 *Phys. Rev. B* **73** 193107
- [20] Giaque W F and Stout J W 1936 *J. Am. Chem. Soc.* **58** 1144–1150
- [21] McGreevy R L and Pusztai L 1988 *Molecular Simulation* **1** 359–367
- [22] Tucker M G, Keen D A, Dove M T, Goodwin A L and Hui Q 2007 *J. Phys. Cond. Mat.* **19** 335218
- [23] Shoemaker D P, Seshadri R, Hector A L and Tachibana M *ArXiv e-prints* **1101.0791v1**
- [24] Toby B H 2001 *J. Appl. Cryst.* **34** 210–213
- [25] Peterson P F, Gutmann M, Proffen T and Billinge S J L 2000 *J. Appl. Cryst.* **33** 1192
- [26] Jepsen O and Andersen O K 1995 *Z. Phys. B Condensed Matter* **97** 35–47
- [27] Seshadri R, Baldinozzi G, Felser C and Tremel W 1999 *J. Mater. Chem.* **13** 2829
- [28] Becke A D and Edgecombe K E 1990 *J. Chem. Phys.* **92** 5397
- [29] Silvi B and Savin A 1994 *Nature* **371** 683
- [30] Galy J, Meunier G, Andersson S and Åström A 1975 *J. Solid State Chem.* **13** 142–159
- [31] Kobayashi H, Kanno R, Kawamoto Y, Kamiyama T, Izumi F and Sleight A W 1995 *J. Solid State Chem.* **114** 15–23
- [32] Johnson M B, James D D, Bourque A, Dabkowska H A, Gaulin B D and White M A 2009 *J. Solid State Chem.* **182** 725–729
- [33] Zeller R C and Pohl R O 1971 *Phys. Rev. B* **4** 2029–2041
- [34] Liu X and v Löhneysen H 1996 *Europhys. Lett.* **33** 617
- [35] Safarik D J, Schwarz R B and Hundley M F 2006 *Phys. Rev. Lett.* **96** 195902